
Geometric Optical Illusions

*A thesis submitted in partial fulfillment of the
requirements for the award of the degree of*

Master of Sciences

by

Mainak Mandal

(12MS092)

Department of Mathematics and Statistics

IISER Kolkata

Supervisor

Dr. Kuntal Ghosh

*Center for Soft Computing Research,
Indian Statistical Institute, Kolkata*

Co-Supervisor

Dr. Satyaki Mazumder

*Department of Mathematics & Statistics,
IISER Kolkata*



INDIAN INSTITUTE OF SCIENCE EDUCATION AND RESEARCH KOLKATA

APRIL, 2017

DEDICATION

This thesis work is dedicated to my parents, Sri Balaram Mandal and Smt. Alpana Mandal.

AUTHOR'S DECLARATION

I hereby declare that this thesis is my own work and, to the best of my knowledge, it contains no materials previously published or written by any other person, or substantial proportions of material which have been accepted for the award of any other degree or diploma at IISER Kolkata or any other educational institution, except where due acknowledgement is made in the thesis. I certify that all copyrighted material incorporated into this thesis is in compliance with the Indian Copyright (Amendment) Act, 2012 and that I have received written permission from the copyright owners for my use of their work, which is beyond the scope of the law. I agree to indemnify and save harmless IISER Kolkata from any and all claims that may be asserted or that may arise from any copyright violation.

April 2017
IISER Kolkata

Mainak Mandal

CERTIFICATE

This is to certify that the work entitled "Geometric Optical Illusions" embodies the research work done by Mainak Mandal under our joint guidance and supervision for the partial fulfillment of the degree of Master of Science, Indian Institute of Science Education and Research, Kolkata, India. It has not previously formed the basis for the award of any Degree, Diploma, Associateship or Fellowship to him.



April, 2017

Dr. Kuntal Ghosh

Dr. Satyaki Mazumder

IISER Kolkata

Dr. Kuntal Ghosh
Associate Professor
Machine Intelligence Unit
Deputed Faculty
Center for Soft Computing Research
A National Facility
INDIAN STATISTICAL INSTITUTE
203, Barrackpore Trunk Road
Kolkata - 700 108

ACKNOWLEDGEMENT

During the course of writing my MS thesis, many people have been supporting me and my work, and this thesis is a good opportunity to express my gratitude for them.

First of all, I would like to thank my supervisor, Dr. Kuntal Ghosh, for his great support. I believe that this thesis would not have been completed without his expert guidance. I am indebted to him for providing me the plenty of opportunity to explore myself and for teaching me how to be an independent researcher.

Next, I would like to thank my co-supervisor, Dr. Satyaki Mazumder, for the continuous support of my study and research. I thank him for patiently bearing with me for the last one year and believing in my capabilities.

Besides my supervisors, I would like to thank the Department of Mathematics & Statistics IISER Kolkata, for allowing me to carry out this research work outside the institute. I would also like to thank my teachers and collaborators Dr. Arunabha Adhikari(West Bengal State University Barasat), Dr. Debasis Mazumder, Dr. Soma Mitra (CDAC, Kolkata) and Dr. Kamales Bhoumik for all the guidance and discussions from which I have learned a lot.

I am extremely thankful to all my friends at IISER who have helped in making my days enjoyable and fun filled. Prasun, Debanuj, Subhajit, Abhishek , I thank you all for the good times and fun-filled moments. I would also like to thank all my lab-mates at CSCR, ISI Kolkata for helping me with my work whenever needed and for volunteering for the experiments.

Last, but not least, I would also like to thank my parents, who has been a great support during all times.

ABSTRACT

Geometric optical illusions are studied. A basic structure of the visual system is defined. A structures of the underlying perceptual space is developed based on the above definitions. A few well known illusions are studied with assuming this nature of the perceptual space. The model is tested for limitations. The model performs reasonably well for all but contrast illusions. A few ways of solving this limitation are discussed which are present in the literature.

TABLE OF CONTENTS

	Page
Acknowledgement	iv
Abstract	v
List of Tables	viii
List of Figures	ix
1 Introduction	1
2 Definitions	3
2.1 Definitions	3
2.1.1 What Is perception?	3
2.1.2 Visual Perception	3
2.1.3 Early Vision and its Problems	4
2.1.4 How is it solved by Nature?	4
2.1.5 Illusions	4
2.1.6 Geometric Optical Illusions	5
3 Mathematical Model	6
3.1 Mathematical Model	6
3.1.1 Basis of the Model	6
3.1.2 Assumptions for the Model	7
3.1.3 Formulation	7
3.1.4 Distance in Perceptual Field	7
3.1.5 Geodesics in Perceptual field	8
4 Simulations and Results	11
4.1 Simulation of Known Illusions	11
4.1.1 Müller-Lyer Illusion	11
4.1.2 Poggendorff Illusion	15

4.2	Testing the Model	17
4.2.1	LT Joint figure	17
4.2.2	A suspected True Negative figure	18
4.2.3	Baldwin's Illusion	20
5	Experiments and Result Comparison	23
5.1	Experiments	23
5.1.1	Setup and Procedure	23
5.1.2	Results	24
5.2	Result Comparison	27
5.2.1	Comparison with Simulations and Inference	27
6	Discussion and Scope of Future Work	28
	Bibliography	30

LIST OF TABLES

TABLE	Page
4.1 True Negative Figure distortion for different kernel sizes	20

LIST OF FIGURES

FIGURE	Page
3.1 Figure explaining the local coordinate system at O	9
4.1 The Müller-Lyer Illusion	12
4.2 Müller-Lyer Illusion Perceptual Image	13
4.3 The Müller-Lyer Illusion Contour Plot	14
4.4 Müller Lyer Simulation Results	15
4.5 The Poggendorff Illusion Figure	16
4.6 The Poggendorff Contour plot and the simulated Geodesic	16
4.7 The LT joint Figure	17
4.8 The LT joint contour plot	18
4.9 A suspected True Negative figure	18
4.10 True Negative figure Contour	19
4.11 Baldwin’s Illusion	20
4.12 Baldwin’s Illusion Simulation	21
4.13 Baldwin’s Illusion Simulation	21
5.1 Müller Lyer Experiment Data, Subject:Mainak, Right Handed Male, Age: 22	24
5.2 Müller Lyer Experimental Data for different subjects	25
5.3 Müller Lyer Exp, Debasis	25
5.4 Müller Lyer Exp, Kuntal	25
5.5 Müller Lyer Exp, Ashish	25
5.6 Müller Lyer Exp, Soma	25
5.7 Baldwin’s Illusion Experimental Data for different subjects	26
5.8 Baldwin’s Illusion Exp, Ashish	26
5.9 Baldwin’s Illusion Exp, Debashis	26
5.10 Subject:Mainak	26
5.11 Baldwin’s Illusion Exp, Soma	26

INTRODUCTION

Visual information received by the retina is passed on to the lateral geniculate nucleus(LGN), and finally, the information reaches the Visual Cortex. A primary problem for vision psychologists was to determine the extent to which visual perception depends on the raw stimulus. There are two popular paradigms of visual perception found in literature, the top-down processing and the bottom's up processing. The *bottoms-up* paradigm is a data-driven process. It is presumed that the raw stimulus contains all the necessary information and visual perception occurs by processing the raw input by successive structures in the visual pathway. In the *top-down* paradigm visual perception is theorised to be an experience driven process. In the top-down approach, it is assumed that the raw precept is ambiguous, so prior knowledge about the outside world is required to draw an unambiguous inference about the raw stimulus. A major flaw in the bottom-up paradigm is its inability to explain *Visual Illusions*. If the raw precept was truly unambiguous then there would be no scope for misinterpretation, that is to say, there would be no illusions. Visual illusions are a strong evidence in favour of the top-down approach since they affirm that prior knowledge is required for visual perception.

Visual illusions have been studied extensively from the middle of the 19th century. Recently in the field of Computer Vision and Pattern recognition, the study of visual systems of humans and other animals have gained importance due to the fact that biologically inspired models are mostly simple and effective. Visual Illusions are an effective way of studying vision systems since they reveal the prior knowledge built into the vision system. The prior knowledge or the assumptions and biases that any biological vision system uses to draw meaningful insight into the raw stimulus makes it so much better than any human reproduction of a vision system.

In Psychological Research visual illusions are believed to be complex phenomena involving higher order information processing in the visual cortex. As the phenomena occur at the percep-

tual level it is beyond the structure or mechanism of the visual receptors. However, these higher level interactions in the visual cortex are difficult to represent mathematically[3]. But many prominent illusions like the Mach Band illusion, Simultaneous Brightness-contrast Illusion, Grating induction illusion, the Hermann grid illusion and the White effect [5] have been explained satisfactorily on the basis of low-level interactions in the retina and the Lateral Geniculate Nucleus.

In the study of visual space[11][2] by Luneberg and Blank the authors showed that geometry of perceptual space is different from physical space. In fact, they went on to claim using mathematical modelling, that the visual space is, in fact, hyperbolic in nature. The model was based on the evidence provided by Blumenfeld Alley experiment. Although this study was for an unperturbed visual system. That is the alley experiments were performed in the dark without visual cues. And the authors made it clear that they have only checked the evidence for an unperturbed system. Also, the modelling of visual system by Luneberg and Blank was for a binocular system.

In this study, we will study the nature of the perturbed perceptual space[8], where the perturbation is in the form of a visual illusion. We limit our study to geometric visual illusions2.1.6 only. Towards the end of the study we will see that the model can successfully explain many of the known geometric illusions, although it fails in case of a particular kind of geometric illusion namely the contrast illusions4.2.1 we understand qualitatively that why it fails. And we see a few techniques where they solved a similar problem.

DEFINITIONS

2.1 Definitions

Let start off with some definitions first. This is necessary because these terms are sometimes used in layman language and may mean different things to different people. So to avoid misinterpretation it is better to make define things clearly.

2.1.1 What Is perception?

We rarely encounter ambiguity in our daily thought process and perception. Thus it seems to us that our perception of the world is absolute, not open to interpretation. This is because we are not consciously aware of most of the ambiguities that are confronted during the reconstruction of a hypothesis of the physical reality from sensory data. Sensory data is inherently ambiguous, open to many interpretations or hypotheses. There is a strikingly large amount of contribution from the brain that helps us to infer a particular hypothesis(or few, in some rare cases) from sensory data. We are consciously aware of only this inferred hypothesis. So in the words of the 19th-century German psychologist and physicist, Hermann von Helmholtz perceptions are "*unconscious inferences*" about the outside world from sensory data[12].

2.1.2 Visual Perception

Visual perception is the ability to interpret the physical reality by processing information that is contained in visible light. This may be treated as a manageable definition of Visual Perception although our perception of the physical reality is often enriched by input or experience from other sensory organs. For example, our perception of 3-d objects is enriched by the experience from our sense our touch. Thus it is very difficult to separate out and define each form of human

perception individually as they seem to work in perfect symbiosis, enriching our perception of physical reality as a whole. Early vision or Low-level Vision is a set of visual modules that aim to extract a few features about the scene which are essential for scene understanding. High-level visual perception completes the job of producing a coherent interpretation of the image from the features extracted in low-level vision. We are mainly concerned about early vision because we are at a stage where we don't have a proper foundation of early vision so that we can build high-level vision on top of that.

2.1.3 Early Vision and its Problems

The Vision problem as a whole is an inverse problem. We know the effects of the outside world on our retina and we need to find out the causal factors of the effects produced on the retina[14]. This problem is a "*ill-posed problem*" in the sense defined by Jacques Hadamard. A well-posed problem in this notion has to satisfy three properties, namely:

1. A solution exists
2. The solution is unique
3. The solution's behaviour changes continuously with the initial conditions.

In most cases is the solution is not unique, that is a particular retinal image can correspond to many possible scenes in the physical reality. For some cases, the solution is unique but does not vary continuously with the input. For example, edge detection is mainly a problem of numeric differentiation. The problem is ill-posed because the solution doesn't vary continuously with the input[14]. A lot of information is lost while projection of the outside 3-d world into a curved two-dimensional retinal surface. one of the prime reasons why the problem is ill-posed.

2.1.4 How is it solved by Nature?

The principal idea behind solving "*ill-posed*" problems is to restore the "*well-posedness*" in the problem by restricting the space of admissible solutions, by using a suitable "*prior*" information. This process of converting an ill-posed problem into a well-posed one by restricting the solution space is called "*regularisation*". Human visual perception relies on constraints or biases about the physical reality to regularise the early vision problem. So top-down apriori knowledge is essential to provide meaningful insight into retinal images.

2.1.5 Illusions

Richard Gregory aptly stated it "it is surprisingly hard to define '*illusion*' in a satisfactory way"[7]. Although we will consider the following definition for our purpose: When perceptions depart from external world or disagrees with physical reality we experience an illusion. As discussed in

?? our visual system uses apriori assumptions to solve the ill-posed early vision problem. But these assumptions are violated under certain special conditions. So our perception departs from the physical reality under these conditions. Then we experience an illusion. This is one of the principal reasons people study visual illusions. They reveal where the assumptions or biases of the visual system fails. So, in turn, they provide insight into what those assumptions might be. The visual system can be satisfactorily modelled if a sizable number of these biases can be built into a model, or in other words, regularise the vision problem as the visual system does it.

2.1.6 Geometric Optical Illusions

Optical illusions or Visual illusions are a special class of illusions when our visual perception departs from the physical reality. Geometric illusions are a type of optical illusion when geometric properties of the precept differ from physical reality. The geometric properties can be anything shape, size or imaginary extension of a figure. A reason for studying geometric illusions is to understand the geometrical structure of human visual space, and how that structure changes under perturbations. This is a top-down approach objective. Of course, another reason is to understand the role of the low-level vision machinery in causing the illusion. And these cases are suitable for mathematical analysis as the mathematics of geometry of a space is quite well developed and has lots of tools for analysis.

MATHEMATICAL MODEL

3.1 Mathematical Model

In this chapter we are going to discuss the mathematical model that we think is suitable for explaining Geometric Optical Illusions. Firstly, we will see what are the basis for considering such a model. Next, we will move on to the assumptions and formulation of a metric for a perturbed visual space. Finally, we will see how to draw geodesics on this perceptual space, this mimics the process of imagining an extension of a line in the perceptual field.

3.1.1 Basis of the Model

We know that visual information projected on the retina is transmitted to the visual cortex through Lateral Geniculate Nucleus(LGN) finally to the Visual Cortex. On each level of the visual system, each receptor or neuron has connection with some(more than one) receptors in the retina. That is each neuron in the Visual Cortex or the LGN receives signal from a number of receptors in the retina. The receptive field of a receptor or neuron is the region in the visual field which when stimulated creates a response in that particular neuron or receptor. Information required to infer properties of the external world is contained in the relationship between the intensity values of different points in the intensity profile of the stimulus rather than the intensity at an isolated point. This is due to the fact that the intensity profile of the incoming light is an indirect source of information about the objects in the external world. So the relationship between the intensity values between different points provides a clue about the nature of the external world. So it is likely that the retinal intensity image is perceived by the neurons in the visual cortex by interacting with each other[9]. So we assume that the "*perceptual image*" is a function of the retinal intensity image.

3.1.2 Assumptions for the Model

A neuron in the visual cortex can be excited by stimulating a fairly large region in the retina. We assume the state of excitation of the neurons in the visual cortex represents the "perceptual image". We don't claim that this is actually perceived, but analysis of this perceptual image can provide insight or low-level features about the scene. In order to make the analysis easier, we assume that the neural system is uniform, continuous and can be approximated by a linear model. We will try to formulate a metric of the perceptual space based on these assumptions.

3.1.3 Formulation

We consider two Cartesian co-ordinate systems, a (x, y) coordinate system of the field of perception and a (ζ, η) coordinate system of the image. Let a field potential of $g(\zeta - x, \eta - y)$ be induced at a point (x, y) in the field of perception for unit stimuli at a point (ζ, η) on the image. Therefore influence on point (x, y) due to $h(\zeta, \eta)$ on (ζ, η) is $g(\zeta - x, \eta - y) \cdot h(\zeta, \eta)$. Since we assumed the system is linear, superposition of effects of all such (ζ, η) will be the sum of all such effects.

$$(3.1) \quad P(x, y) = q + \int \int h(\zeta, \eta) \cdot g(\zeta - x, \eta - y) \cdot d\zeta \cdot d\eta$$

Where q denotes spontaneous activity. q should change with background brightness and adaptation. Although we assume it to be constant for easier analysis. Relative intensity in the perceptual field represents light and shade of the pattern.

3.1.4 Distance in Perceptual Field

We consider the case when the neural signal passes between two points in the perceptual field. We assume that the signal passes quickly through a region of highly activated neurons in the perceptual field. On the other hand, the signal passes slowly through a region of mildly activated neurons in the perceptual slowly. Taking the above argument into account, it is easy to see that the perceived distance between two points in the perceptual field will be small if the region in between them is highly activated and vice versa. Therefore the perceived distance differs from the physical distance on the image. The unit length on each point of the perceptual field is defined as the length corresponding to a unit length on the image at the corresponding to that point on the image. $D(x, y)$ be the function representing unit distance in the perceptual image. As we discussed in above it should be a function of the perceptual image satisfying the above criterion of distance perception. Therefore:

$$(3.2) \quad D(x, y) = F[P(x, y)]$$

Therefore, the length of a path γ between two points A, B on the perceptual field will be given by:

$$(3.3) \quad D_{AB} = \int_{\gamma} D(x, y) ds$$

This formulation gives us a metric on the perceptual space. Hence we can study the various types of geometric optical illusions. We will analyse different geometric optical illusions and see if the perceived distance from predicted by model matches with what we actually perceive.

3.1.5 Geodesics in Perceptual field

Now we have a metric on the perceptual space. The next thing that we will try to mimic is our capability to extend actual lines with our imagination. Straight lines between two points in any field are *geodesics*, that is a path of minimum distance in that field. Therefore let γ be a path of minimum distance(as calculated in eq:(3.3) between two points on the perceptual field. Now:

$$\begin{aligned} ds &= \sqrt{(dx)^2 + (dy)^2} \\ &= \sqrt{1 + \left(\frac{dy}{dx}\right)^2} dx \end{aligned}$$

Therefore eq:(3.3) can be written as:

$$(3.4) \quad D_{AB} = \int_{\gamma} D(x,y) \sqrt{1 + (y')^2} dx$$

(3.1.5) The integrand of eq:(3.4) is a function of x, y and y' . That is $D_{AB} = f(x, y, y')$. Therefore the path $\gamma(y(x))$ that minimizes the path integral must satisfy the Euler-Lagrange equation(3.5):

$$(3.5) \quad \frac{\partial f}{\partial y} = \frac{d}{dx} \left(\frac{\partial f}{\partial y'} \right)$$

$$(3.6) \quad \Rightarrow \sqrt{1 + (y')^2} \cdot \frac{\partial D}{\partial y} = \frac{d}{dx} \left(D(x,y) \cdot \frac{y'}{\sqrt{1 + (y')^2}} \right)$$

Since x, y and y' are independent till we know the path, that is $y(x)$. Now let the angle between the minimum path and x-axis be ϕ , refer fig:3.1.

$$\begin{aligned} \therefore y' &= \tan(\phi) \\ \Rightarrow \sin(\phi) &= \frac{y'}{\sqrt{1 + (y')^2}} \end{aligned}$$

(3.8)

So using substituting eq:3.7 in eq:3.6 we get:

$$(3.9) \quad \frac{\partial D}{\partial y} = \frac{d}{ds} (D(x,y) \cdot \sin(\phi))$$

The equation $D(x,y) = c$ represents a plane curve in the (x,y) plane. Let $'O'$ be a point on the geodesic. We define the direction of the x-axis at the point $'O'$ to be in the direction of the normal to the curve $D(x,y) = c$ at the point $'O'$. The the normal to $D(x,y) = c$ at $'O'$ is given by $\nabla D(x,y)|_{O'}$.

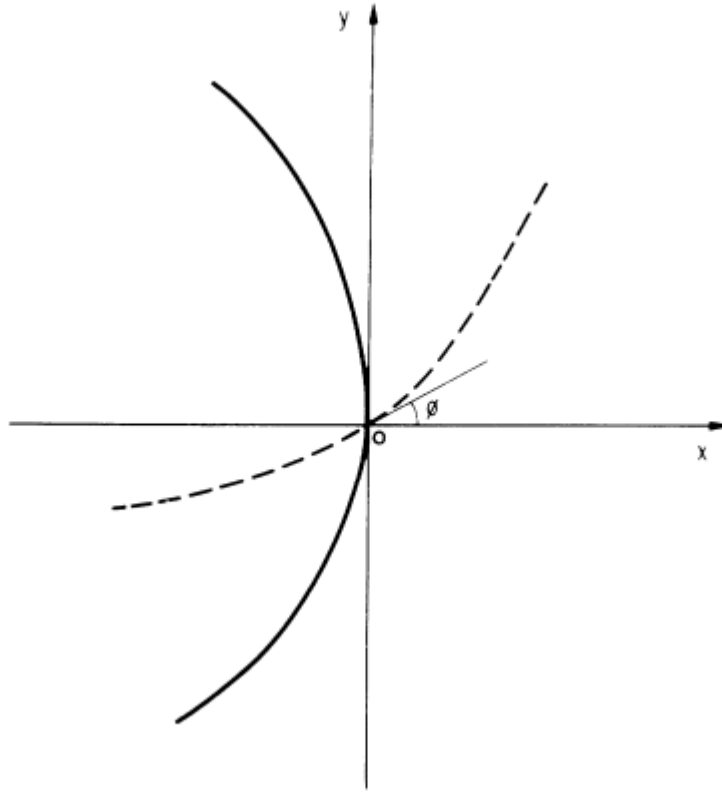


Figure 3.1: Figure of the plane curve ($D(x, y) = c$) and the geodesic. the continuous line denotes the plane curve and the dashed line denotes the geodesic.

$$\begin{aligned} \nabla D(x, y) &= k \cdot \hat{i} \\ \Rightarrow \frac{\partial D}{\partial y} &= 0 \end{aligned}$$

From eq:3.10 and eq:3.9 we have:

$$(3.10) \quad \frac{d}{ds} (D(x, y) \cdot \sin(\phi)) = 0$$

$$(3.11) \quad \therefore D(x, y) \cdot \sin(\phi) = \text{constant}$$

A neuron in the perceptual space receives information from a fairly large retinal region, this is called the *receptive field* of that neuron. We assume that the receptive field of a neuron is similar to the receptive field of a on-center off-surround retinal ganglion cell. Therefore the

spatial coupling function $g(\zeta - x, \eta - y)$ is given by:

$$(3.12) \quad g(\zeta - x, \eta - y) = \frac{k_1}{2\pi\sigma_1^2} \exp \left[-\frac{(\zeta - x)^2 + (\eta - y)^2}{2\sigma_1^2} \right]$$

$$(3.13) \quad -\frac{k_2}{2\pi\sigma_2^2} \exp \left[-\frac{(\zeta - x)^2 + (\eta - y)^2}{2\sigma_2^2} \right]$$

If a neuron has this kind of center-on surround-off receptive field, then it is excited if the receptive cells in the centre of the field are stimulated and are inhibited if the peripheral cells are stimulated. The spatial filtering function for the off-center on-surround cells could also be considered in this case but the mathematical representation would have been quite similar. The retinal ganglion cells are located on the inner surface of the retina, and they are the first neurons in the visual pathway.

Now everything is in place except for the function mention in eq:3.2. From the discussion in section 3.1.4 it can be easily seen that the simplest function that satisfies the above mention criteria is the inverse function. Therefore:

$$(3.14) \quad F[P(x, y)] = \frac{1}{P(x, y)}$$

$$(3.15) \quad \Rightarrow D(x, y) = \frac{1}{P(x, y)}$$

Now we can explicitly calculate the distance between two points and draw the imaginary extension of a real line on the perceptual field. In the next chapter, we will study some know geometric illusions using this structure of the perceptual space.

SIMULATIONS AND RESULTS

4.1 Simulation of Known Illusions

In this chapter, we are going to start with simulation of some known illusions like the Müller-Lyer Illusion and the Poggendorff Illusion. Then we will test the model for defects. Finally, we will see that it seems that the model fails to explain a class of illusions known as the *contrast illusions*. We are not so sure due to lack of experimental evidence.

4.1.1 Müller-Lyer Illusion

The *Müller-Lyer Illusion* is one of the best known Geometric illusion, which is being studied since its discovery in the end of the 19th century. In its present form, the figure consists of a pair of stylised arrows. The longer straight line segments are called the "*shafts*" of the arrows, while the shorter line segments protruding from the end of the shafts are called the "*wings*". The end with outward wings is called a "*tail*" and the one with inward wings is called a "*head*". The angle between the shaft and the wings is called the *fanning angle*. So the fanning angle for a head end is acute and that for a tail end is obtuse. The figure 4.1 is the demonstration of the illusion.

When viewers are asked to compare the length of the shafts of the two arrows, they perceive the line segment above with *tails* at both ends to be longer than the line segment with the *heads* at both ends. In both the cases we consider the length of shaft, but the presence of the wings create a distortion of our sense of length.

There is another form of the same illusion, the form in which it was first devised. The illusionary figure consists of a shaft with a head and a tail and the viewers are asked to place a marker in the centre of the shaft. They invariably place it closer to the tail end. Nevertheless, we will study the illusion in its present form only, because the mathematical analysis is more or less

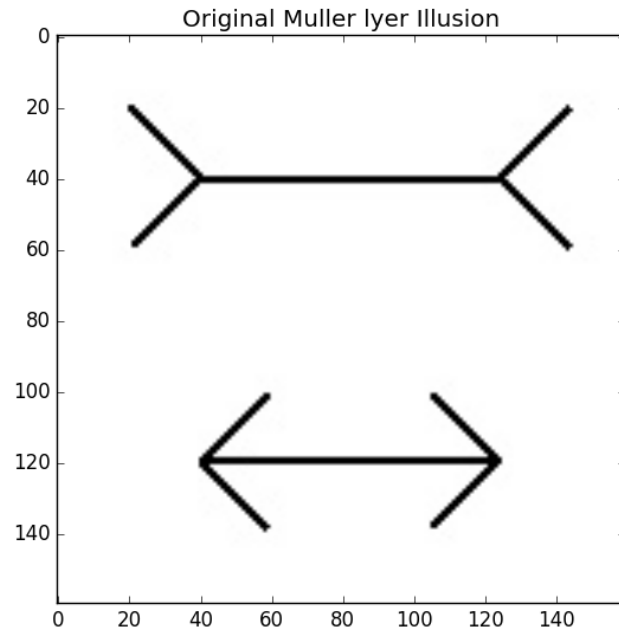


Figure 4.1: The Müller-Lyer Illusion

the same.

Now let us get down to how the simulation is performed. The perceptual image, $P(x, y)$ is obtained from the original Müller-Lyer image by convolving the image with the DOG spatial filtering function. Figure 4.2 represents the perceptual image. Where the input image has size 200x200 pixels. The function used for filtering is $g(\zeta - x, \eta - y)$ as described in equation (3.12).

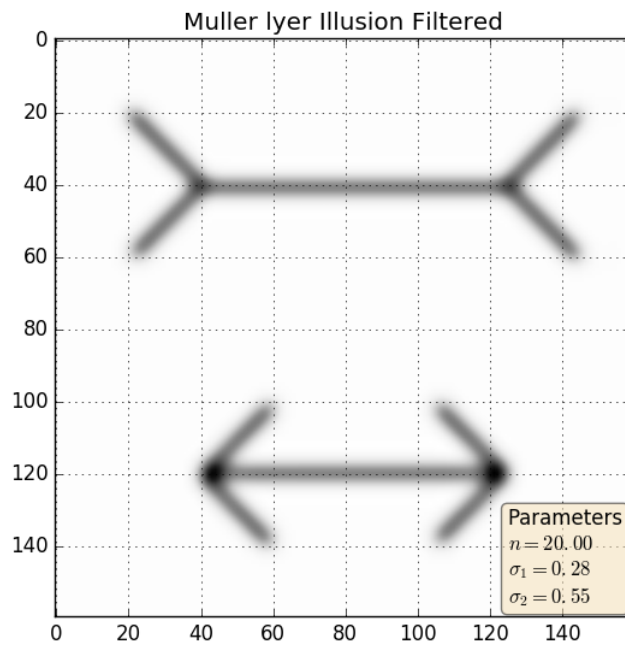


Figure 4.2: Müller-Lyer Illusion Perceptual Image

For the simulations we have taken the following constants:

- $k_1 = 1$
- $k_2 = 1$
- $\sigma_1 = .28$
- $\sigma_2 = 0.55$
- $2n + 1$ is the kernel width. $n = 20$.
- ζ, η varies between n to $-n$ for each (x, y) .

The contour plot of the perceptual image is shown in the figure4.3 The length of the shafts in

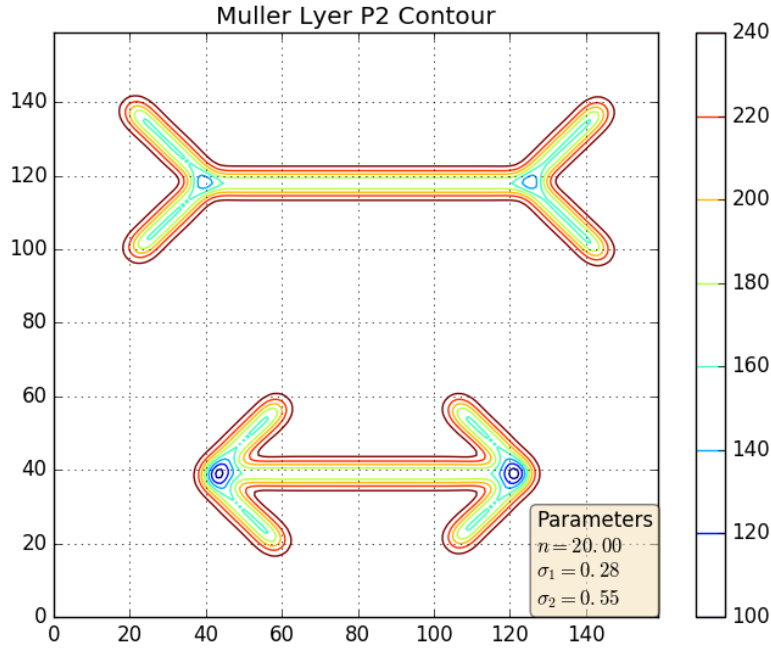


Figure 4.3: The Müller-Lyer Illusion Contour Plot

both the cases was calculated by taking a path integral over the line segment with the potential of the perceptual field, as per eq:3.4. The end-points of the path integral was chosen manually by locating (eye estimation) the centre of the maxima near the end of the shaft in the contour plot of the perceptual image. The integral over the head figure will be smaller than the tail figure. In a sample run with the above parameters, the difference in length between two illusionary figures of fanning angle 45° and 135° was found to be around 15% of the average perceived length of the two shafts. The shaft of the figure with fanning angle of 45° had a smaller perceived length than the 135° one. To investigate the illusion in detail we performed the simulation on various Müller Lyer figures by modifying the fanning angle, i.e. the angle between the shaft and the wings. The

fanning angle(angle between the shaft and the wings) was varied between 15° to 165° in 15° intervals. The results of the simulation are shown in figure:4.4.



Figure 4.4: Müller Lyer Simulation Results

In figure4.4 we can see that the percentage deviation(the deviation between the Müller Lyer shaft and control line of the same length as a percentage of the length of the control line) is a increasing function of the fanning angle. In the next chapter we will see some experimental data, which will show that this is actually the case, qualitatively.

4.1.2 Poggendorff Illusion

This is a very simple Geometric Optical Illusion, that involves the misperception of the position of one segment of a transverse line that has been interrupted by the contour of an intervening structure. In its present form, it consists of a pair of vertical straight line segments, intersected by a slanting line segment. But the slanting line is not continued in-between the two parallel lines. For better visualization refer to figure4.5. In this figure, it seems as if the two parts of the slanting straight lines are not part of the same straight line but this is not the case. It was discovered in the late 19th century. Although it is not so well studied as the Müller-Lyer Illusion but it is suitable our purpose. The theory developed in section3.1.5 of extending straight lines with imagination in the perceptual field can be tested on this illusion.

Firstly the perceptual image was created by convolution with the spatial filtering mentioned in equation(3.12). Then the drawing of the imaginary line on the Poggendorff figure was simulated using the iteration condition derived in the equation 3.11. Starting with an initial point on the

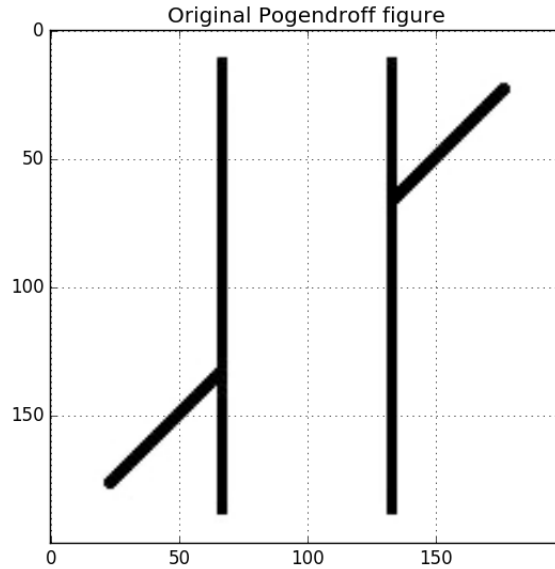


Figure 4.5: The Pogendorff Illusion Figure

slanting line, where the direction of the geodesic and the local coordinates is known. Then a small step is taken in the direction of the geodesic and the ϕ at that point is calculated. The angle ϕ is relative to the local coordinates of the second point. From ϕ at the second point, the direction of the geodesic at that point can be calculated. The iteration can be continued in this way to calculate the path of the geodesic on the perceptual image. The contour plot of the perceptual image along with the geodesic is shown in figure 4.6.

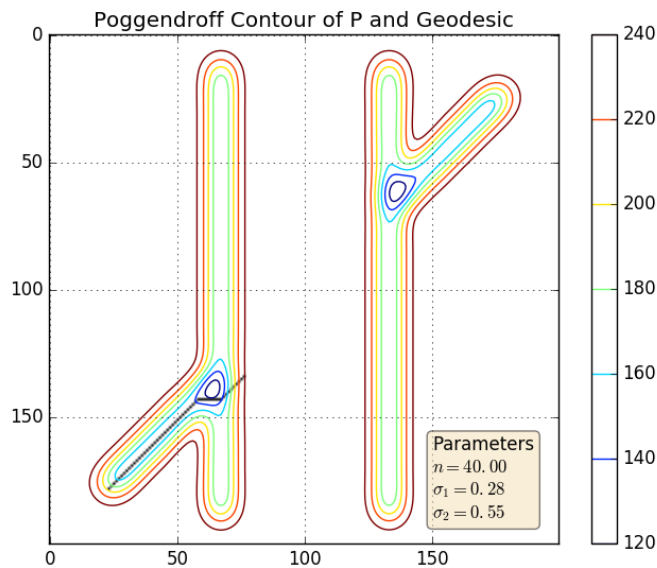


Figure 4.6: The Pogendorff Contour plot and the simulated Geodesic

From the results of the simulation, it can be seen that at the junction with the parallel lines the geodesic bends away from the "straight" path. So it can be said that the imaginary extension of the slanting line bends away from the "straight line" in the euclidean sense. This also matches with what is reported in literature.

4.2 Testing the Model

From the above discussion, we can easily deduce that the model works satisfactorily on some well-known illusions. But this doesn't fully establish the validity of the model. It needs to be tested on some non-illusionary figures and some other types of illusions. For this purpose we will use a figure:4.7 and a geometric illusion of contrast figure [10], as shown in figure:4.9 . The human visual system doesn't perceive an illusion in the 1st figure but we suspect that the present model might fail in this case. And the second figure produces a sense of illusion in the human visual system but it is suspected that the present model will not be able to detect the illusion since it ignores the effect of long-range illusions.

4.2.1 LT Joint figure

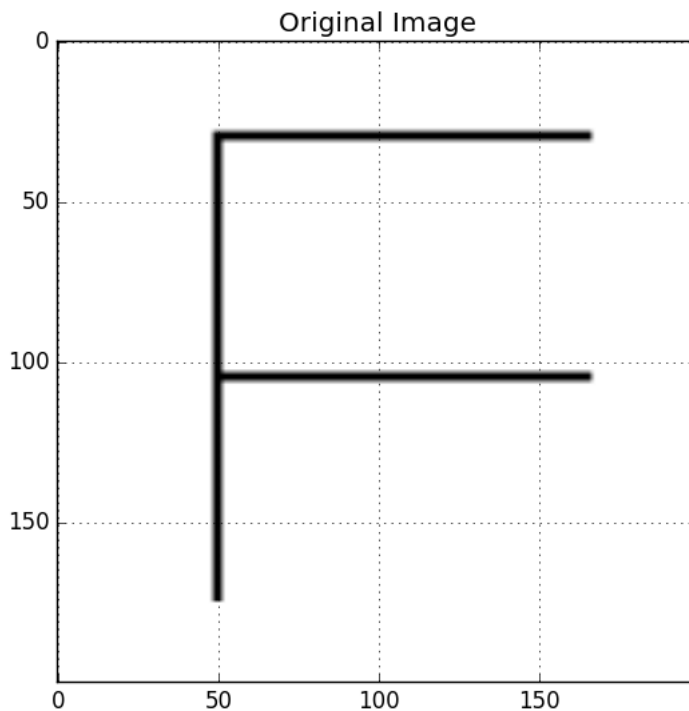


Figure 4.7: The LT joint Figure

The stimulus consists of an 'F' like figure, of which both the arms are of the same length. But the arms are connected to the vertical shaft by two different type of joints. The upper arm is

connected by an 'L' type joint and the lower arm is connected by a 'T' type joint. Since the present model takes into account the local interactions for estimating the perceptual length so it is legitimate to suspect that the estimated length of arms will be different. The contour plot of the perceptual image along with the parameters used for simulation is shown below.

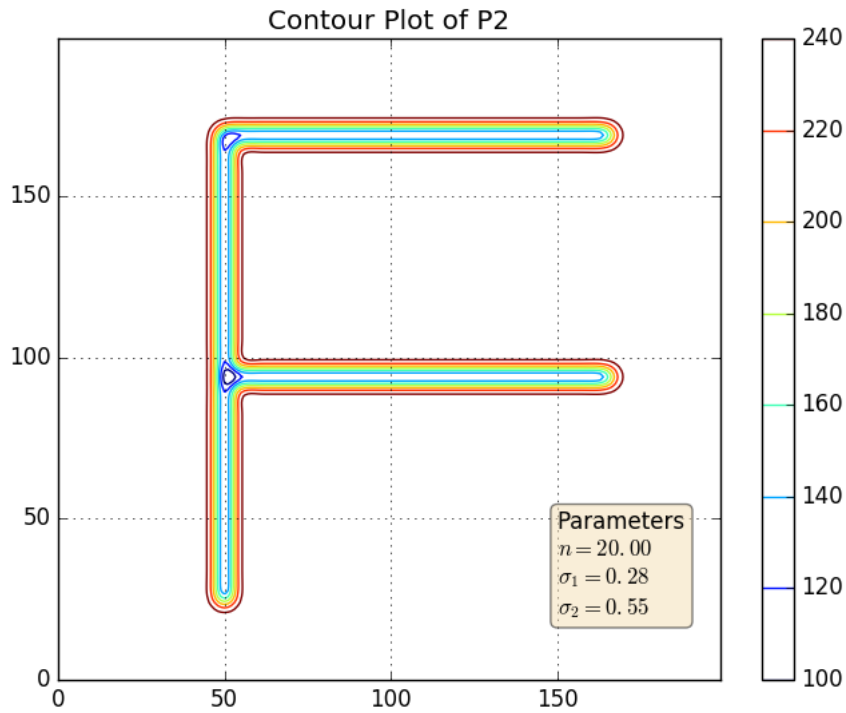


Figure 4.8: The LT joint contour plot

The length of both the arms were estimated as explained in the Müller-Lyer Illusion analysis. The difference in length was not significant (around 0.1-0.2% for reasonable kernel sizes), that is it was within the numerical error bounds. Hence the model survived the test as it predicted the length of the two different arms to be same, as a normal human being would see. So we can conclude that the present model is a close approximation of the human visual system in this case.

4.2.2 A suspected True Negative figure



Figure 4.9: A suspected True Negative figure

This illusion is not a well studied named illusion, although it is quite well suited for our purpose. This has been described as an illusion of contrast in [10]. In this context, contrast implies contrast of size. In simple words, parts adjacent to large extents appear smaller and parts those adjacent to smaller extents appear larger. The figure consists of a horizontal line segment with vertical notches at four points. Two notches the ends and two notches at middle separated by a constant distance, only the length of the horizontal line segment differs in the two figures. This distorts our length perception. The distance between the two notches is same in both the figures. But we perceive the distance between the notches in the left-hand side figure in 4.9 to be smaller than the same in the right-hand side figure. Next, the image was analysed as previously described. The contour plot of the perceptual image along with the parameters used in the simulation is shown below.

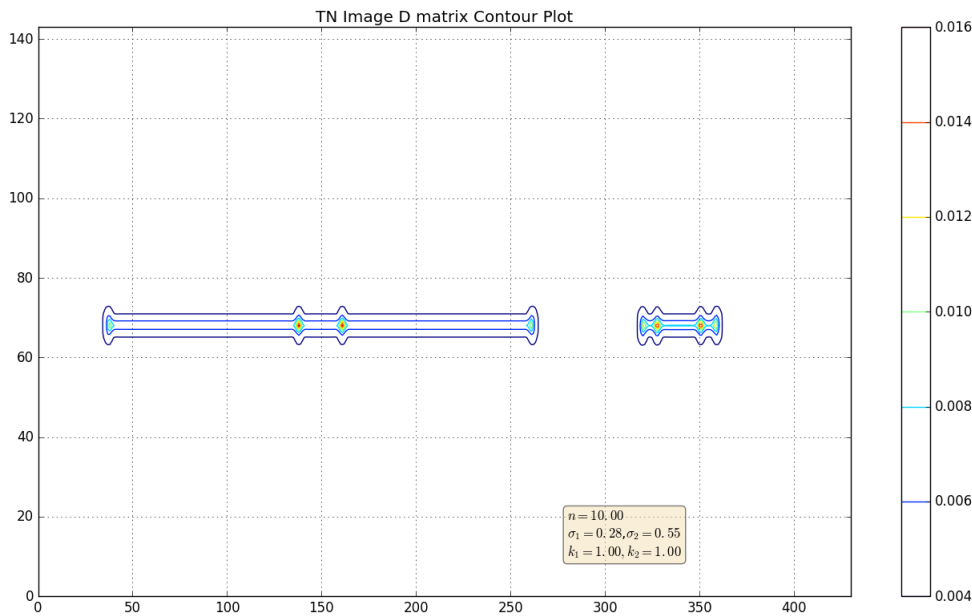


Figure 4.10: True Negative figure Contour Plot

The perceptual distance was measured between the two middle notches for both the figures. The difference in length as percentage of the mean length seemed to be too small (0.5%) for what we perceive. Although it was in the right direction i.e. the figure with the smaller arms had longer perceptual length. Different kernel sizes were used in the simulation to see if the effect was different for different kernel sizes. Table: ?? shows the variation of the difference in length with kernel size. The difference in length never rose above 1.5% of the mean length, which again is too small compared to the level of distortion in lengths we perceive.

On being confronted with this disparity, it became necessary to investigate other illusion of this kind i.e., illusions of contrast. A notable illusion of this kind is Baldwin's illusion.

Kernel size(n)	Difference in length(%)
10	0.51
15	1.45
20	0.85
25	0.84
30	0.69
35	0.69
40	0.65
45	0.64

Table 4.1: True Negative Figure distortion for different kernel sizes

4.2.3 Baldwin's Illusion

Baldwin illusion was first discovered by Baldwin (Baldwin, 1895). In this illusion, the apparent length of the standard line is altered by the presence of the flanking squares. The size of the squares influences the apparent length of the line between the squares. This is a contrast illusion in the sense discussed in subsection:4.2.2. This illusion is similar to the previous illusion because in both cases the disparity in perceived length seems to be caused by presence of different sized extents. The illusion in its current form is shown below:

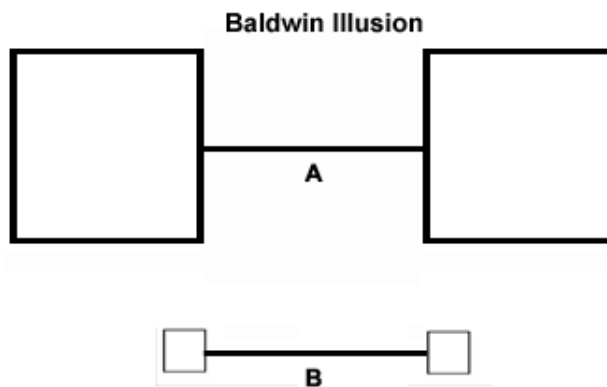


Figure 4.11: Baldwin's Illusion

The shafts of both the objects in figure:4.11 are of the same length but the presence of the flanking squares create a distorted perception that the shaft of object 'A' is smaller than that of object 'B'.

The process of analysis of this figure was similar to the process previously stated. First, the perceptual image was plotted and the end points of the perceptual distance measurement program were determined. Then the perceptual lengths of the shafts were computed. The difference in length between the two shafts as percentage of the mean length was seemed too small in comparison to the level of distortion perceived by the human visual system.

To investigate the issue further, the effects for the Baldwin's figure with different square sizes were simulated. The input image consisted of the Baldwin's figure and a control line of same

pixel length as the shaft of the Baldwin's figure. This is illustrated in figure:4.12

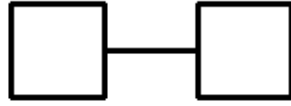


Figure 4.12: Baldwin's Illusion Simulation Figure

The disparity between the perceptual length of the shaft and the control line was measured. The results of the simulation are presented below in a graphical format.

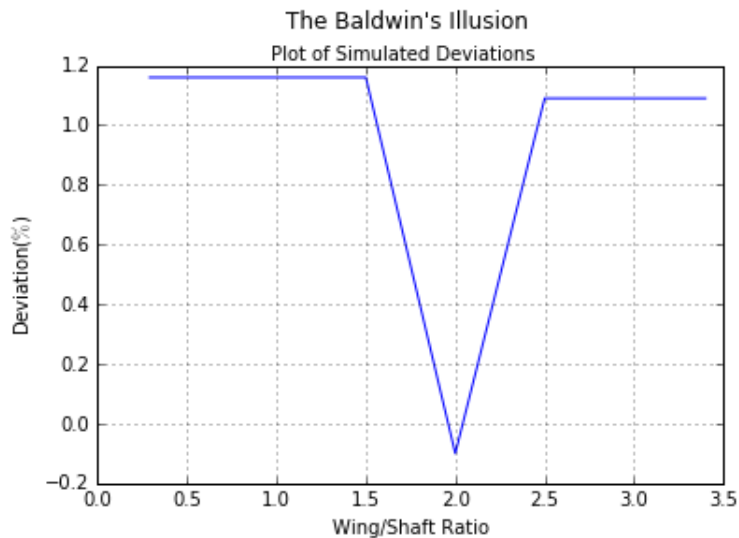


Figure 4.13: Baldwin's Illusion Simulation Figure

On the X-axis is the size of the side of the squares as a fraction of the shaft length. And on the Y-axis is the deviation in perceptual length between shaft and the control line segment as a percentage of the latter. Form the plot it can be deduced that the results are not in agreement with what is expected. The deviation is expected to be a more or less increasing function of the wing/shaft length ratio. We tried to compare our results with actual experimental findings in literature. But no such study with freely available data set could be found. So we decided to conduct our own experiment and determine the actual nature of the curve. In the next chapter

we will discuss the experimental procedure ,setup and outcome of the experiment. Then we will be in a better position to comment on the accuracy of the model.

EXPERIMENTS AND RESULT COMPARISON

5.1 Experiments

Psychophysics can be described as the study of relationship between stimuli and perception. In psychophysical experiments, experimenters seek to ascertain if the subject can identify a stimulus, differentiate it from another or describe the magnitude or nature of the difference. In this experiment focus on visual stimuli and measure the magnitude of distortion produced by certain illusion causing stimuli. The experiments were repeated several times for each subject because human perception is subjective i.e., it depends upon context and ambiance, so it fluctuates. As previously mentioned we will investigate the Müller Lyer Illusion and the Baldwin's Illusion in detail, so that we can compare those with the prediction of the model.

5.1.1 Setup and Procedure

The experimental setup is rather simple and the experimental conditions are described in detail so that the setup can be accurately reproduced. The setup consists of a LCD monitor, chin rest and a keyboard for data entry by the subject. The distance between the monitor and the chin rest was adjusted to be 70cm. This seemed to be the most comfortable viewing distance while testing the setup. Ambient light didn't seem to affect the results of the experiments, so we conducted all the experiments in normal lighting conditions. The stimulus figures were 400x400 pixels in size with a white background in the standard 1024x768 pixel display. The stimulus generation was done using Python Imaging Library and the data logging part was done using 'Psycopy', an open source python platform[13]. The subjects were shown a image and there was a adjustable reference line. The task was to look at the image and set the length of the reference line equal to the image. The initial length of the reference line was set at random between 22 pixels \pm

shaft length. In each run, a subject was to repeat this task for 23 stimuli, 11 Müller Lyer illusion figures and 12 Baldwin's illusion figures.

5.1.2 Results

5.1.2.1 Müller-Lyer Experiment

In the Müller Lyer figures the fanning angle(angle between the shaft and the wings) was varied between 15° to 165° in 15° intervals. All the 11 figures were shown one by one in a random order and the subjects were asked to set the reference line equal to the shaft length in each case. The Müller Lyer figures had 176px shaft length and 56 pixels wing length. The experiment was repeated for each stimulus three times to minimize the chances of human error in perception. The result of the experiment is shown in figures:5.1 and 5.2.

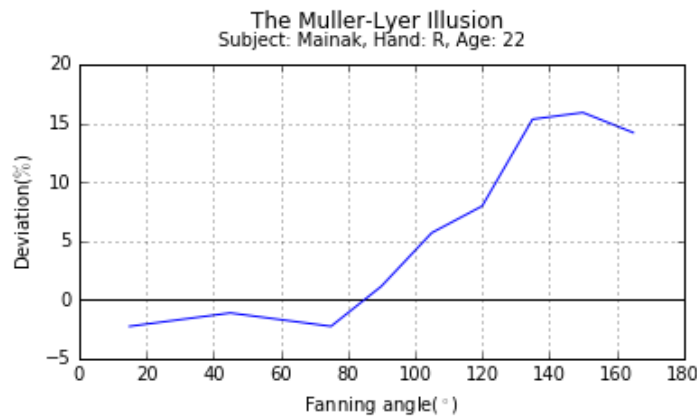


Figure 5.1: Müller Lyer Experiment Data, Subject:Mainak, Right Handed Male, Age: 22

From the figures:5.1 and 5.2 we can see that the percentage deviation increases as a function of the fanning angle. This is the normal expected behavior in case of Müller Lyer Illusion.

Figure 5.2: Müller Lyer Experimental Data for different subjects

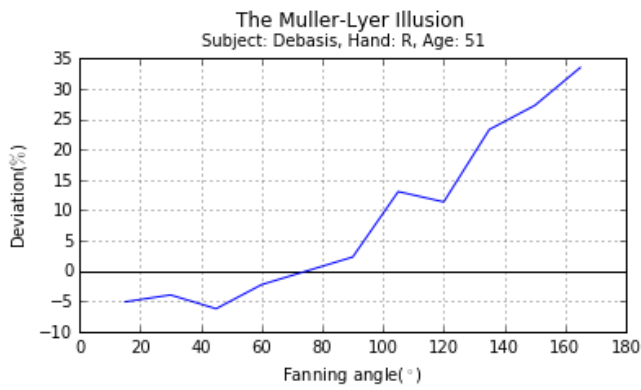


Figure 5.3: Subject: Debasis

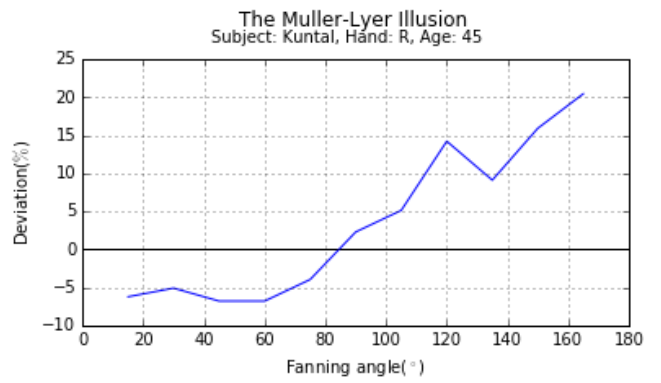


Figure 5.4: Subject: Kuntal

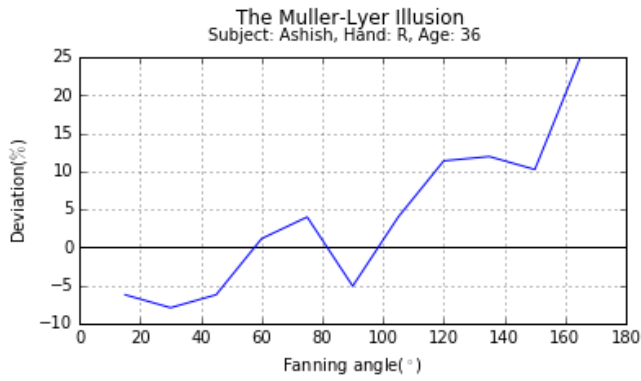


Figure 5.5: Subject: Ashish

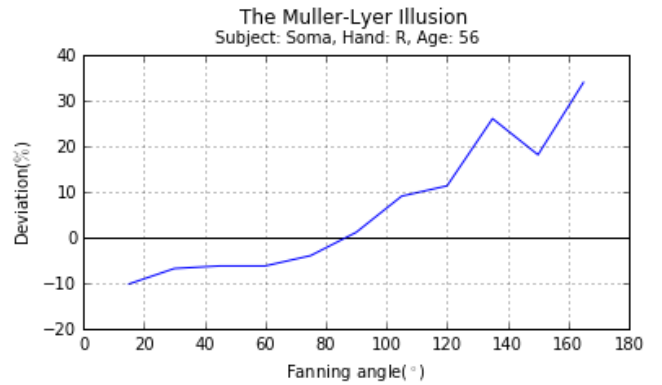


Figure 5.6: Subject: Soma

5.1.2.2 Baldwin's Experiment

The Baldwin's experiment was similar, in this case the Müller Lyer were replaced by the Baldwins figure and the size of the flanking squares were varied. The subjects were asked to adjust the reference line equal to the shaft length in each case. The shaft length for the Baldwin's figures was fixed at 50px for all the figures. The results of the experiment is shown in figure:5.7.

Figure 5.7: Baldwin's Illusion Experimental Data for different subjects

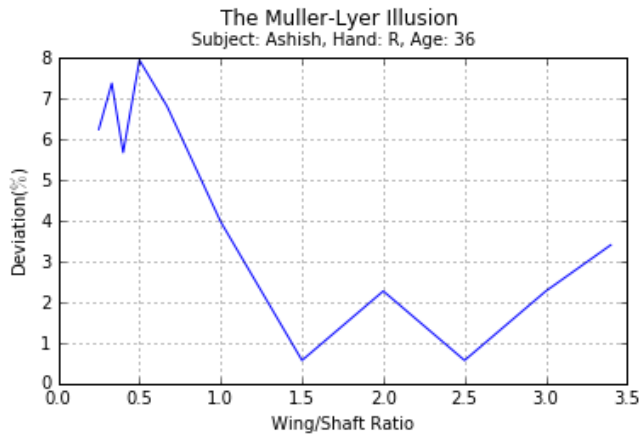


Figure 5.8: Subject: Ashish

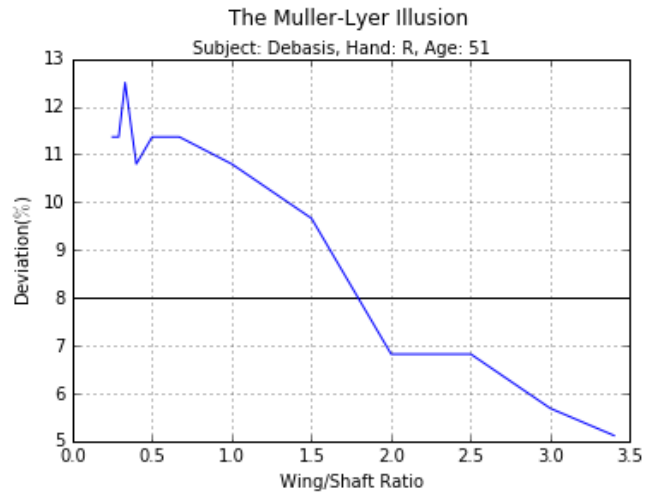


Figure 5.9: Subject: Debasis

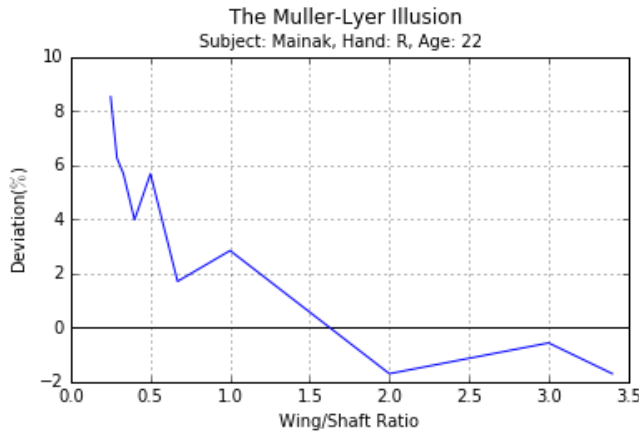


Figure 5.10: Subject: Mainak

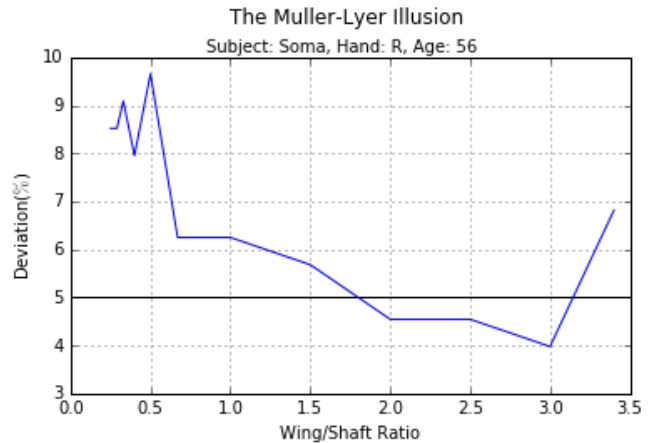


Figure 5.11: Subject: Soma

From the figures:5.7 we can see that the percentage deviation decreases as a function of wing/shaft ratio. Though the behaviour of the curve seems a bit erratic, this can be rectified by repeating the experiment with the same subjects. At least this is what was observed with subject Mainak.

5.2 Result Comparison

5.2.1 Comparison with Simulations and Inference

The results of the simulation of the same set of figures is shown in section 4.13 and 4.4. Comparing both set of plots it can be seen that the simulation results match qualitatively match with the experimental results in the Müller Lyer case. But in the Baldwin's illusion the simulation predictions do not tally with the experimental results.

Thus we can infer that the present model failed to take in to account some of the influential factors causing the Baldwin's illusion.

DISCUSSION AND SCOPE OF FUTURE WORK

We have established that the current model works predicts the some geometric optical illusions really well, whereas fails to take into account the causal factors for a group of illusions namely the contrast illusions. So now we are going to address the issue of solving this discrepancy in the present model. For that purpose we looked up on available literature in this field, to know what are the ways people have attempted to solve this kind of problems. While doing this we came across some interesting pieces of literature.

The most notable work seems to be done by a mathematician named Rodolf.K.Luneberg[11], which was continued by Albert.A.Blank after his death. This was as early as the 1950's. Luneberg and Blank formulated a metric for the unperturbed Visual Space, and determined that the Visual space not inherently euclidean, in particular it is hyperbolic. This formulation was based on the findings of the parallel alley experiment by Blumenfeld. This is a rich and well formulated theory, with a sound mathematical backing.

A recent paper in this approach by Werner Ehm et al.[4], have modelled geometric optical illusion as superposition of "context" and "target". The perception of the target depends on the context. They have satisfactorily explained the Ehrenstein-Orbison type illusions using the Poincare's model of 2-d hyperbolic geometry. They have also tested their predicted results by performing a pilot experiment. Though this is a interesting development this has models do not claim to model the human visual system directly. Or in other words they don't take a bottoms up approach, rather they deal with that top down approach of high level vision. This is not a problem in the true sense, we can always apply high level vision processing on whatever low level features we have.

We have also come across some promising work in the field of low level vision modelling, that is directly connected to how the biological machinery of vision works. K.Ghosh[6] and A.

Bakshi[1] have successfully explained brightness assimilation effects using a Extended Classical Receptive Field. The contrast illusions of size are in a sense negative assimilation, the presence of larger extents nearby decreases the size of the object in comparison to the control and vice versa. So this model has some promise of solving the discrepancy. Another interesting feature of this model is that it is very close to the model we already have so the present model can be easily modified to this model to check if it works or not.

BIBLIOGRAPHY

- [1] A. BAKSHI AND K. GHOSH, *Perceiving and modelling brightness contradictions through the study of brightness illusions*, in *New Directions in Paraconsistent Logic*, Springer, 2015, pp. 447–463.
- [2] A. A. BLANK, *The luneburg theory of binocular visual space*, *JOSA*, 43 (1953), pp. 717–727.
- [3] J. CHAO, Y. MIYATA, S. YOSHIDA, M. SUZUKI, AND T. KISHIGAMI, *Realization of geometric illusions using a lateral-inhibitive shifting model and intrinsic geometry of subjective visual space*, *Electronics and Communications in Japan (Part III: Fundamental Electronic Science)*, 86 (2003), pp. 1–10.
- [4] W. EHM AND J. WACKERMANN, *Geometric–optical illusions and riemannian geometry*, *Journal of Mathematical Psychology*, 71 (2016), pp. 28–38.
- [5] K. GHOSH, S. SARKAR, AND K. BHAUMIK, *A possible explanation of the low-level brightness–contrast illusions in the light of an extended classical receptive field model of retinal ganglion cells*, *Biological Cybernetics*, 94 (2006), pp. 89–96.
- [6] ———, *A possible explanation of the low-level brightness–contrast illusions in the light of an extended classical receptive field model of retinal ganglion cells*, *Biological Cybernetics*, 94 (2006), pp. 89–96.
- [7] R. L. GREGORY, *Eye and brain: The psychology of seeing*, no. 1, Princeton university press, 2015.
- [8] N. KAWABATA, *Mathematical analysis of the visual illusion*, *IEEE Transactions on systems, man, and cybernetics*, 6 (1976), pp. 818–824.
- [9] T. LINDBERG, *A computational theory of visual receptive fields*, *Biological cybernetics*, 107 (2013), pp. 589–635.
- [10] M. LUCKIESH, *Visual illusions: Their causes, characteristics and applications*, D. Van Nostrand Company, 1922.
- [11] R. K. LUNEBURG, *The metric of binocular visual space*, *JOSA*, 40 (1950), pp. 627–642.

- [12] D. MUMFORD, *Pattern theory: the mathematics of perception*, arXiv preprint math/0212400, (2002).
- [13] J. W. PEIRCE, *Psychopy: psychophysics software in python*, *Journal of neuroscience methods*, 162 (2007), pp. 8–13.
- [14] T. POGGIO AND C. KOCH, *Ill-posed problems in early vision: from computational theory to analogue networks*, *Proceedings of the Royal Society of London B: Biological Sciences*, 226 (1985), pp. 303–323.